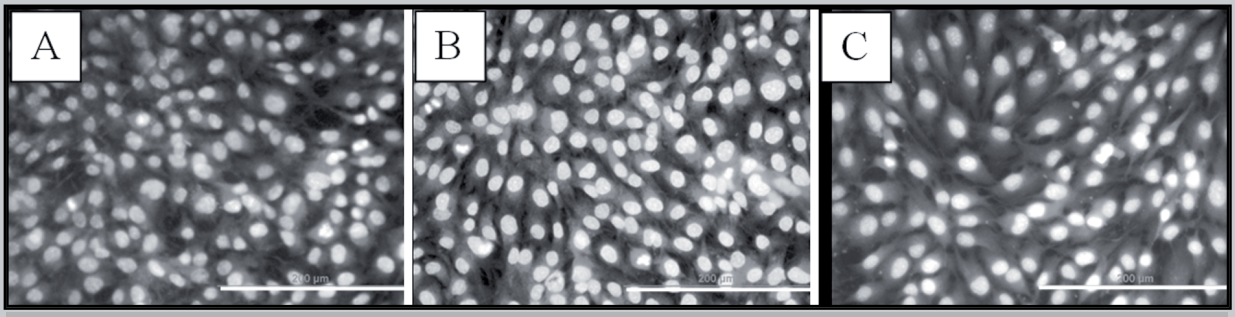

FIG. 1. Morphology of human osteoblast-like MG 63 on day 4 after seeding on titanium (A), on stainless steel (B), and on the control polystyrene culture dish (C). Cells stained with Texas Red C2-Maleimide and Hoechst #33342. Olympus IX 51 microscope, obj. 20, DP 70 digital camera, bar = 200 µm.

cytotoxicity kit for mammalian cells (Invitrogen, Molecular Probes, USA).

The larger samples (30x30 mm) were inserted into GAMA polystyrene dishes (diameter 5 cm; GAMA Group Joint-Stock Company, Ceske Budejovice, Czech Republic) and seeded with 300000 cells/dish (approx. 15300 cells/cm^2) suspended in 9 ml of the above mentioned culture medium. These samples were used for evaluating the cell number on days 1, 4 and 7 after seeding, using a Beckman Vi-CELL XR Cell Analyser automatic cell counter.

The results indicated that the number of initially adhering cells on day 1 after seeding was significantly lower on the titanium (5320±390 cells/cm^2) and on the stainless steel (4110±370 cells/cm^2) than on the control polystyrene culture dishes (7740±350 cells/cm^2). However, on day 4 after seeding, the cell population density on both metallic materials studied here became significantly higher than on the control polystyrene dishes (75200±2 890 cells/cm^2 on Ti and 90870±2 350 cells/cm^2 on steel vs. 56440±1180 cells/cm^2 on polystyrene). This suggests faster cell proliferation on both metallic materials than on polystyrene. At the same time, the cell number on the stainless steel samples was significantly higher than on the Ti samples. On day 7, the differences in number of adhered cells on both studied metals and on the control polystyrene substrate was on an average similar (from 328780±680 cells/cm^2 to 362 200±760 cells/cm^2). The cell viability on all tested materials was almost 100% in all culture intervals. The morphology of the cells on the studied materials was similar to the morphology of the adhered cells on the control polystyrene dishes, i.e. the cells were mostly flat and polygonal, and the size of their cell spreading areas was similar on all tested materials. The cells were distributed homogeneously on the entire material surface, and on day 4 they started to form confluent cell layers (FIG.1).

It can be concluded that the tests of biocompatibility confirmed that the titanium and the stainless steel promoted the adhesion and growth of bone-derived cells, and thus these materials are promising for construction of bone implants and for their good integration with the surrounding bone tissue. Further studies on osteogenic cell differentiation, potential immune activation and the response of the bone cells to growth factors, including bone morphogenetic protein, are in progress.

Acknowledgements

Supported by the Technological Agency of the Czech Republic (grant No. TA01011141) and by the Grant Agency of the Czech Republic (grant No. P108/10/1858). We also thank Mr. Robin Healey (Czech Technical University, Prague) for his language revision of the text.

[Engineering of Biomaterials, 109-111, (2011), 10-11]

BIOAPATITE MADE FROM CHICKEN FEMUR BONE

Monika Šupová[1], Gražyna Simha Martynková[2], Zbyněk Sucharda[1], Tomáš Suchý[1,3]

[1] Czech Academy of Sciences,
nstitute of Rock Structure and Mechanics,
Department of Composites and Carbon Materials,
Prague, Czech Republic,
supova@irsm.cas.cz
[2] VŠB-Technical University of Ostrava,
Nanotechnology Centre,
Ostrava-Poruba, Czech Republic
[3] Czech Technical University in Prague,
Fac. of Mechanical Eng., Prague, Czech Republic

[Engineering of Biomaterials, 109-111, (2011), 11-13]

Introduction

The inorganic part of the human bone has chemical and structural similarities with hydroxyapatite (HA) in the form of plate-shaped nanocrystals that are 2–3 nm in thickness and tens of nanometers in length and width [1]. Bones do not have a pure or a stoichiometric HA but incorporate many elements; some of them at the ppm level [2]. Ionic substitution can affect the crystal structure, crystallinity, surface charge, solubility etc., leading to major changes in the biological performance upon implantation. Nano HA was successfully synthesized from biowaste chicken eggshells and from different types of sea creatures. Another possible source for preparation of bioapatite (BAP) can be warm-blooded animal bones (e.g. bovine bone) [3]. In this study we report a preparation and characterization of bioapatite from chicken femur, such as another alternative source of bone apatite.

Materials and methods

BAP sample was obtained using a chemical and thermal deproteinating process inspired by Murugan et al. [3]. The cortical chicken bones were heated with a 2% NaCl aqueous solution at 150°C and pressure of 0.2 MPa in autoclave followed by disintegration of the sample in mixer. Then the degreasing process in acetone – ether mixture (ratio 3:2) for 24 hours followed. Bone samples were then treated with 4% NaOH solution at 70°C for 24 hours. The chemically treated bone samples were calcined overnight at 500°C. Product was washed with deionized water and dried in oven at 80°C. Sodium and magnesium were determined by AAS method (Varian AA 240), phosphate by the photometric method (UV-VIS 500, Unicam) and calcium by titration method. Specific gravity was determined pycnometrically in water. Morphology of BAP particles was studied by TEM (Tecnai G2 Spirit Twin). The surface area was determined by the BET method (Sorptomatic 1990) with nitrogen as the adsorbate gas. The XRD pattern of the final nanopowder was obtained with X-Ray Powder Diffractometer D8 Advance (Bruker AXS, Germany), Bragg-Brentano diffraction geometry with CoK radiation (λ=1.78 Å), position sensitive VANTEC detector, reflecting mode. The crystallite size and distribution was calculated using software MudMaster using Warren-Averbach [4] approach. The FTIR spectroscopy was done with Protégé 460 E.S.P. (Thermo-Nicolet, Inc., USA) by KBr tablet technique. The CO_3^{2-} content was qualitatively determined from the infrared spectrum by comparing the extinction coefficient (E) of the 1450 cm^{-1} (carbonate) and 569 cm^{-1} (phosphate) bands using the formula: $\%CO_3^{2-}=13.5(E1450/E569)-0.2$ [3], the CO_3^{2-} content was also quantitatively determined using an el. analysis by a CHNS/O microanalyzator Flash FA 1112 Thermo Finnigan (Carlo Erba).

Results and discussions

BAP sample contents 0.71 and 0.80 wt.% of magnesium and sodium, respectively. The amount of magnesium in apatite is usually much higher than that incorporated into its crystalline structure and it is mainly adsorbed on the apatite crystal surface [5]. Owing to these substitutions the Ca/P molar ratio is smaller (1.64) than 1.67 that is typical for stoichiometric HA. This fact becomes evident also in value of specific gravity 2.864 for BAP sample compared to 3.080 for stoichiometric HA. Generally, the nanoparticles appear to have a needle-shape (FIG.1a) with heights of ~ 20 nm to 90 nm and diameters of ~ 13 nm to 20 nm. The average values of the specific surface area (73.3 $m^2 \cdot g^{-1}$) and pore specific volume (0.28 $cm^3 \bullet g^{-1}$) determined by BET demonstrate the nano nature of BAP particles.

The FTIR spectrum (FIG.1b) shows a weak broad bands ranging between 3600-3350 cm^{-1} and at 1634 cm^{-1} corresponds to strongly adsorbed and/or bound H_2O. The weak 3564 cm^{-1} band corresponds to the OH^- group, other bands correspond to OH^- group at 635 and 595 cm^{-1} were not detected which is in agreement with published data [6]. The low portion of OH^- groups in the bone apatite thus would enable

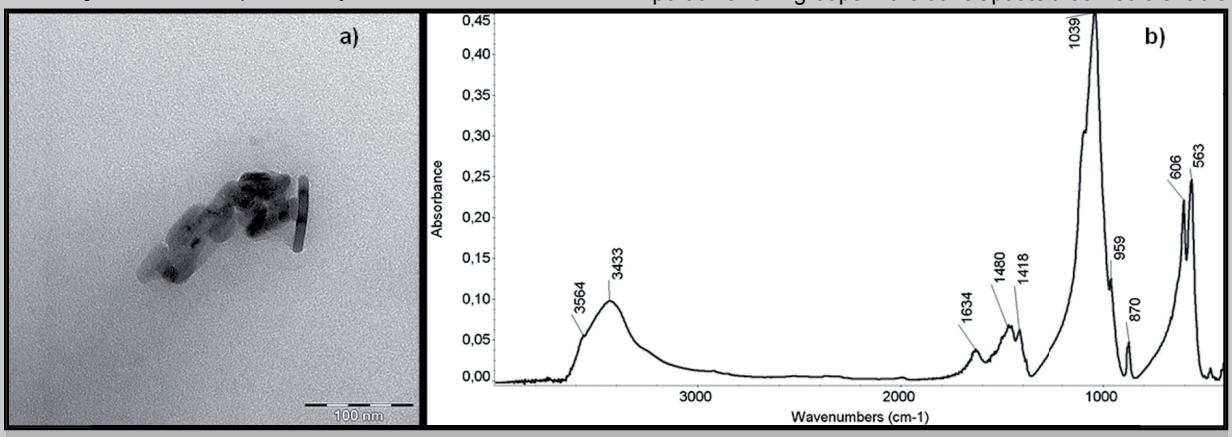

FIG. 1. TEM image (a), baseline corrected FTIR spectrum (b) of BAP sample.

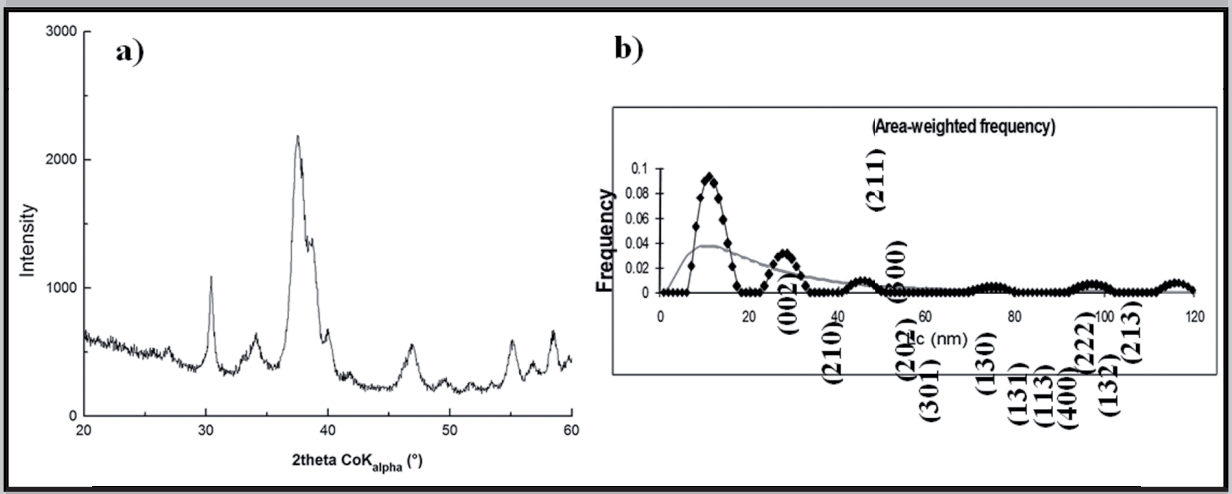

FIG. 2. XRD pattern (a) and crystallite size distribution (b) of BAP sample.

its dissolution. A strong band of PO_4^{3-} group was seen at 1039, 959 (stretching vibration) and bands at 590–610 cm^{-1} regions are due to deformation vibration of PO_4^{3-} ions. Bands pertain to the B-type CO_3^{2-} functional group at ~ 1450 and 870 cm^{-1}, indicating the substitution of CO_3^{2-} ions into the apatite. The CO_3^{2-} peak at 1550 cm^{-1} assigned to the A-type was not detected owing to none existence of OH^-. The amount of CO_3^{2-} estimated by a FTIR method using an equation given in the Materials and Methods was found to be 3.11 wt.%, which corresponds well with the results determined by CHNS/O analyzer-3.25 wt.%. Carbonates in apatite correlates positively with its solubility [7].

XRD analysis served for material crystallinity estimation. The diffraction pattern of BAP (FIG.2a) represents typical broadened peaks of semi-crystalline material. The area-weighted mean crystallite size <Lc> was calculated according to the theory of Warren and Averbach [4] from distribution <Lc>=27 nm. The crystallite size distribution curve has two major maximums (FIG.2b) and calculated log-normal distribution (solid line) roughly traces the character of the BAP distribution. Majority of the crystallites is in range 12 to 18 nm. Larger domains are represented with sizes around 30 nm. The crystallites are rather small and uniform, which is advantageous for further applications. For comparison, the average crystallite size Lc of human bone, studied by Handschin et al. [8], has been determined as 28 nm within age group 0-25, to reach a constant average domain size of 34 nm within age group 30-80. Crystallite size is connected with apatite solubility and resorbability in bone [7].

Conclusions

The chicken femur bone was used to isolate nano-bioapatite powder via chemical treatment followed by calcination. XRD, BET, crystalite size distribution and TEM proved the nanostructured character of the sample. Values of specific gravity and Ca/P molar ratio together with chemical analysis and FTIR spectrometry have demonstrated that BAP sample was Ca-deficient with Na, Mg and carbonate substitutions. Properties mentioned above are related to good solubility and resorbability, which are very important for bone remodeling. The present study shows that chicken femur bone can be effectively utilized for the preparation of nano-bioapatite powders as potential filler to biocomposites.

Acknowledgements

This study was supported by the Czech Science Foundation (No. 106/09/1000), and by Ministry of Education project Transdisciplinary Research in Biomedical Engineering II. (No. MSM 6840770012).

References

[1] Weiner S., Wagner H.D.: Annu. Rev. Mater. Sci. 1998; 28: 271-98.
[2] Skinner H.C.W.: Mineralogical Magazine 2005; 69: 621-41.
[3] Murugan R., Ramakrishna S., Panduranga Rao K.: Mater. Lett. 2006; 60: 2844-47.
[4] Warren B.E., Averbach B.L.: J. Appl. Phys. 1953; 21: 595-599.
[5] Bertoni E., Bigi A., Cojazzi G., Gandolfi M., Panzavolta S., Roveri N.: J. Inor. Biochem. 1998; 72: 29-35.
[6] Pasteris J.D., Wopenka B., Valsami-Jones E.: Elements 2008; 4: 97-104.
[7] Wopenka B., Pasteris J.D.: Mat. Sci. Eng. C-Bio S 2005; 25: 131-143.
[8] Handschin R.G., Stern W.B.: Bone 1995; 16: 355S-363S.

RESULTS FOR MODERN BANDAGING MATERIALS APPLICATION IN ALVEOLITIS TREATMENT

Shevela T.L., Pohodenko-Chudakova I.O., Groshev E.Y.

Belarusian State Medical University,
Belarusian Collaborating Center EACMFS,
220025, Minsk,
Kossmonavtov str., 9 – 1 – 63, PO Box 286.
Republik of Belarus,
ip-c@yandex.ru

[Engineering of Biomaterials, 109-111, (2011), 13-14]

Introduction

A small pain appears in the postoperative wound after the tooth extraction and when the anesthesia effect is not active. Its intensity depends on the operation severity. Alveolitis is forming after the alveolar socket injury and its gum crushing as a result of the postoperative treatment disturbance when the blood clot is washed out from the alveolar socket during the mouth wash. Microorganisms of the oral cavity penetrate into it and provoke its inflammation [1, 2].

Food ingress into the alveolar socket, not keeping of the oral cavity hygiene also provoke the alveolitis development. This complication is due to the following factors: periodont tissues injuries of the extracted tooth when the microcirculation is violated into it; infected tooth into the alveolar socket, dental deposit; infection-inflammatory focus in the region of the apical or marginal periodontitis; reduction of the activity level of the of the antimicrobial local system of the oral cavity protection. An iodoform turunda was used by surgeon-stomatologist during long time for treatment of alveolitis during surgery hours. This preparation had good recommendations as a banding material used for many years. But the turunda manufacture is a complicated process because not all pharmaceutical products are available. Iodoform turunda contains of diethyl ether, glycerin, anesthesin powder, iodophor, 70% alcohol, which are not used for alcohol production for medical purposes. Special equipment is required for this medicine storage - vessel in dark glass with lapped head. Now Borisov Plant for Medical Preparations produces banding materials such as «Diosept», «Kombiksin», «Protzelan» (FIG. 1). Above-stated confirms the topicality of this subject.

Aim of the work was to make comparative research and evaluation of the banding materials «Diosept», «Kombiksin», «Protzelan» effectiveness. In order to realize this aim we emphasized next subjects:

1) to appreciate application effectiveness of the banding material of «Kombiksin» in maxillofacial surgeon practice;
2) to appreciate application effectiveness of the banding material of «Diosept» in maxillofacial surgeon practice;
3) to appreciate application effectiveness of the banding material of «Protzelan» in maxillofacial surgeon practice;
4) to make comparative assessment of the banding materials application during the treatment of alveolitis.

Objects and methods

We made clinical examination of 32 patients with alveolitis during September, 2010 - April, 2011 in the Minsk Central Region Polyclinic Nr 14. All patients were divided into groups